

**Production, crystallization and preliminary X-ray diffraction of the Gas  $\alpha$ -helical domain in complex with a nanobody**

Triest, Sarah; Wohlkönig, Alexandre; Pardon, Els; Steyaert, Jan

*Published in:*

Acta Crystallographica Section F - Structural Biology Communications

*DOI:*

[10.1107/S2053230X14020962](https://doi.org/10.1107/S2053230X14020962)

*Publication date:*

2014

*Document Version:*

Final published version

[Link to publication](#)

*Citation for published version (APA):*

Triest, S., Wohlkönig, A., Pardon, E., & Steyaert, J. (2014). Production, crystallization and preliminary X-ray diffraction of the Gas  $\alpha$ -helical domain in complex with a nanobody. *Acta Crystallographica Section F - Structural Biology Communications*, 70(11), 1504-1507. <https://doi.org/10.1107/S2053230X14020962>

**Copyright**

No part of this publication may be reproduced or transmitted in any form, without the prior written permission of the author(s) or other rights holders to whom publication rights have been transferred, unless permitted by a license attached to the publication (a Creative Commons license or other), or unless exceptions to copyright law apply.

**Take down policy**

If you believe that this document infringes your copyright or other rights, please contact [openaccess@vub.be](mailto:openaccess@vub.be), with details of the nature of the infringement. We will investigate the claim and if justified, we will take the appropriate steps.

Sarah Triest,<sup>a,b</sup> Alexandre  
Wohlkönig,<sup>a,b</sup> Els Pardon<sup>a,b</sup> and  
Jan Steyaert<sup>a,b\*</sup>

<sup>a</sup>Structural Biology Brussels, Vrije Universiteit  
Brussel (VUB), Pleinlaan 2, 1050 Elsene,  
Belgium, and <sup>b</sup>Structural Biology Research  
Center, Vlaams Instituut voor Biotechnology  
(VIB), Pleinlaan 2, 1050 Elsene, Belgium

Correspondence e-mail: jan.steyaert@vub.ac.be

Received 6 August 2014

Accepted 19 September 2014

## Production, crystallization and preliminary X-ray diffraction of the Gαs α-helical domain in complex with a nanobody

GPCR–G-protein complexes are one of the most important components of cell-signalling cascades. Extracellular signals are sensed by membrane-associated G-protein-coupled receptors (GPCRs) and transduced *via* G proteins towards intracellular effector molecules. Structural studies of these transient complexes are crucial to understand the molecular details of these interactions. Although a nucleotide-free GPCR–G-protein complex is stable, it is not an ideal sample for crystallization owing to the intrinsic mobility of the Gαs α-helical domain (AHD). To stabilize GPCR–G-protein complexes in a nucleotide-free form, nanobodies were selected that target the flexible GαsAHD. One of these nanobodies, CA9177, was co-crystallized with the GαsAHD. Initial crystals were obtained using the sitting-drop method in a sparse-matrix screen and further optimized. The crystals diffracted to 1.59 Å resolution and belonged to the monoclinic space group  $P2_1$ , with unit-cell parameters  $a = 44.07$ ,  $b = 52.55$ ,  $c = 52.66$  Å,  $\alpha = 90.00$ ,  $\beta = 107.89$ ,  $\gamma = 90.00^\circ$ . The structure of this specific nanobody reveals its binding epitope on GαsAHD and will help to determine whether this nanobody could be used as crystallization chaperone for GPCR–G-protein complexes.

### 1. Introduction

Heterotrimeric guanine nucleotide-binding proteins (G proteins) control many cellular processes by playing an important role in signal transduction (Simon *et al.*, 1991; Hamm, 1998). G proteins are generally activated by G-protein-coupled receptors (GPCRs) upon binding of a ligand, and transduce the extracellular signal in the cell to start a cascade of intracellular responses (Oldham & Hamm, 2008). All G proteins consist of three subunits ( $G\alpha$ ,  $G\beta$  and  $G\gamma$ ), where  $G\alpha$  is responsible for nucleotide binding and  $G\beta\gamma$  forms an obligate functional dimer. G-protein activation occurs when GDP is exchanged for GTP in the  $G\alpha$  subunit. This cyclic process is catalysed by guanine nucleotide-exchange factors (GEFs), of which GPCRs are the most studied example. When a GPCR is activated by an extracellular signal, conformational changes trigger GDP release from the  $G\alpha$  subunit and a stable nucleotide-free GPCR–G-protein complex is formed (Rasmussen, DeVree *et al.*, 2011). Upon binding of GTP in the nucleotide-binding pocket,  $G\alpha$  undergoes conformational changes which lead to its dissociation from the GPCR. This also causes the tightly associated G-protein heterotrimer to separate and free both  $G\alpha$ –GTP and  $G\beta\gamma$ , which will regulate downstream effector molecules (Bohm *et al.*, 1997). The intrinsic GTP hydrolase activity of  $G\alpha$  resets the G protein to its basal state, where GDP-bound  $G\alpha$  reassociates with the  $G\beta\gamma$  heterodimer. The  $G\alpha$  subunit itself is composed of two domains: a Ras-like GTPase domain that hydrolyses GTP and a unique helical domain. Recently, structural studies revealed that the α-helical domain (AHD) acts as a lid that traps the nucleotide in a binding pocket. In the absence of a bound nucleotide, the AHD is a flexible switch that adopts a broad range of possible positions (Westfield *et al.*, 2011).

To promote the stabilization of GPCR–G-protein complexes in the nucleotide-free form, nanobodies were generated that bind and preferably stabilize the GαsAHD. Nanobodies (Nbs) or VHHs are the small antigen-binding fragments (15 kDa) of heavy-chain-only antibodies (hcAbs) found in Camelidae (Muyldermans *et al.*, 2001;

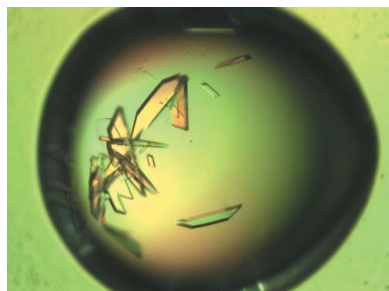


**Table 1**  
Macromolecule-production information.

	G $\alpha$ sAHD	CA9177
Source organism	<i>Bos taurus</i>	<i>Lama glama</i>
DNA source	Synthetic	Synthetic
Expression vector	pQE-60	pMESy4
Expression host	<i>E. coli</i> BL21 (DE3)	<i>E. coli</i> WK6 (su-)

Muyldermans, 2013). They specifically recognize native conformations and can reduce complexity or flexibility of proteins by trapping the protein in one particular conformation (Steyaert & Kobilka, 2011). In recent years, immune libraries have been exploited to select nanobodies that can be used as crystallization aids (Pardon *et al.*, 2014). This approach has been especially successful in the determination of crystal structures of GPCRs in their active states (Rasmussen, Choi *et al.*, 2011; Kruse *et al.*, 2013) and of GPCR-G-protein complexes (Rasmussen, DeVree *et al.*, 2011). As a continuation of this strategy, additional nanobodies were generated that target the AHD of G $\alpha$ s. The aim was to reduce the observed mobility of the AHD (Westfield *et al.*, 2011), which causes heterogeneity of a GPCR-G-protein sample and is one of the challenges to overcome when crystallizing such complexes. Additionally, these nanobodies could serve as imaging tools to unravel the conformational changes and signalling mechanisms of GPCR-G-protein complexes in living

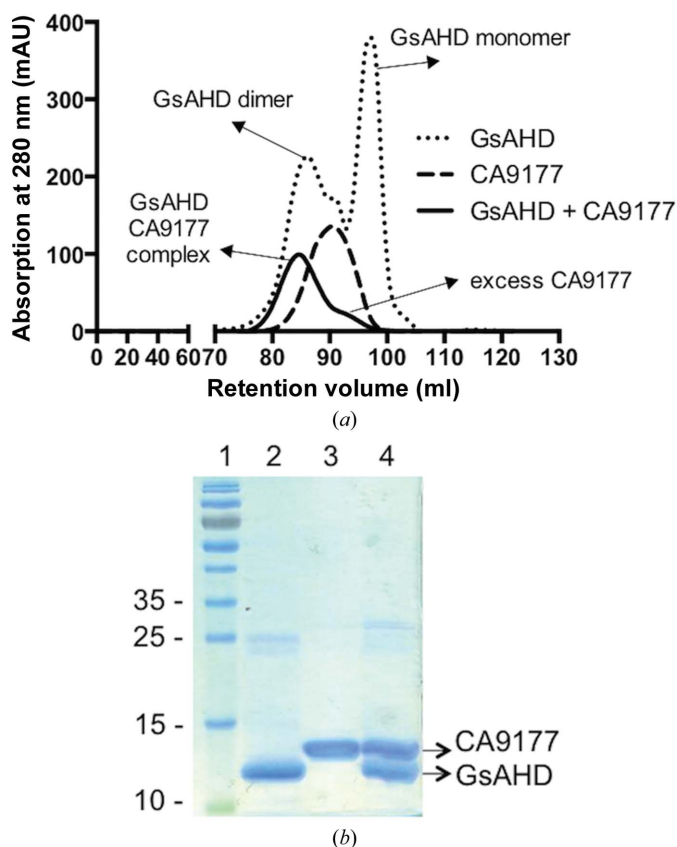


**Figure 1**  
G $\alpha$ sAHD-CA9177 complex purification. (a) Gel-filtration elution profile of G $\alpha$ sAHD-CA9177 complex compared with free G $\alpha$ sAHD and CA9177. A Superdex 75 16/60 column was equilibrated with 50 mM Tris pH 8.0, 150 mM NaCl, 2 mM DTT. (b) Concentrated fractions were loaded onto a 15% SDS-PAGE gel and stained with Instant Blue. Lane 1, PageRuler Prestained Protein Ladder (Thermo Scientific); lane 2, G $\alpha$ sAHD (14.7 kDa); lane 3, CA9177 (13.4 kDa); lane 4, G $\alpha$ sAHD-CA9177 complex.

cells (Irannejad *et al.*, 2013; Irannejad & von Zastrow, 2014). Here, we report the crystallization of a G $\alpha$ sAHD-Nb (CA9177) complex.

## 2. Materials and methods

### 2.1. Production and purification of G $\alpha$ sAHD in complex with a nanobody

**2.1.1. Expression and purification of G $\alpha$ s  $\alpha$ -helical domain.** The expression vector for the purification of the AHD of bovine G $\alpha$ s (P04896) was a kind gift from Roger Sunahara's laboratory (Table 1). The DNA sequence of G $\alpha$ sAHD was cloned into a pQE-60 expression vector, which introduces a C-terminal His<sub>6</sub> tag and contains an ampicillin-resistance gene. The plasmid was transformed into chemically competent *Escherichia coli* BL21(DE3) cells. For expression, 1 l Terrific Broth (TB) containing 100  $\mu$ g ml<sup>-1</sup> ampicillin was inoculated with 10 ml of an overnight preculture. Cells were grown at 310 K with shaking (120 rev min<sup>-1</sup>) until they reached an OD<sub>600</sub> of 0.7–1.1. Induction was performed by adding 1 mM isopropyl  $\beta$ -D-1-thiogalactopyranoside (IPTG) and lowering the temperature to 293 K for overnight expression of recombinant G $\alpha$ sAHD.

Cells were harvested by centrifugation for 10 min at 6000g. The pellet was resuspended in 20 ml lysis buffer [50 mM Tris pH 8.0, 100 mM NaCl, 2 mM  $\beta$ -mercaptoethanol (BME), 200  $\mu$ M phenylmethylsulfonyl fluoride (PMSF), 50  $\mu$ g ml<sup>-1</sup> DNase, 20 mM MgCl<sub>2</sub>] per litre pellet. The solubilized cells were lysed at 138 MPa using a cell disruptor (Constant Systems) and centrifuged for 45 min at 40 000g. The clarified supernatant was loaded onto a 5 ml nickel-nitrilotriacetic acid (Ni-NTA) column (HisTrap HP, GE Healthcare) equilibrated with 50 mM Tris pH 8.0, 100 mM NaCl, 2 mM BME, 200  $\mu$ M PMSF, 10 mM imidazole. G $\alpha$ sAHD was eluted with five column volumes (CV) of 50 mM Tris pH 8.0, 100 mM NaCl, 2 mM BME, 200  $\mu$ M PMSF, 250 mM imidazole. The protein was further purified on a Superdex 75 HR 16/60 column equilibrated with 50 mM Tris pH 8.0, 150 mM NaCl, 2 mM DTT. The G $\alpha$ sAHD-containing fractions were concentrated (Amicon Ultra, MWCO 3000, Millipore) to a minimal concentration of 10 mg ml<sup>-1</sup>, flash-frozen and stored at 193 K.

**2.1.2. Nanobody expression and purification.** For production and purification, the DNA sequence encoding the nanobody was cloned into the *E. coli* expression vector pMESy4 (Pardon *et al.*, 2014; Table 1). The nanobody is expressed with a C-terminal His<sub>6</sub>-EPEA tag (De Genst *et al.*, 2010) and a pelB signal peptide directs the recombinant nanobody to the periplasm. The plasmid was transformed into the *E. coli* WK6 expression strain and a fresh colony was used to start a preculture in 50 ml Luria-Bertani broth (LB), 100  $\mu$ g ml<sup>-1</sup> ampicillin, 2% glucose. For large-scale production, 1 l TB was supplemented with 100  $\mu$ g ml<sup>-1</sup> ampicillin, 2% glucose, 1 mM MgCl<sub>2</sub> and inoculated with 10 ml overnight-grown preculture. The cultures were grown at 310 K with shaking (120 rev min<sup>-1</sup>) until an OD<sub>600</sub> of 0.6–0.8 was reached. The periplasmic expression of the nanobody was induced by adding 1 mM IPTG for 16 h at 301 K. Cells were harvested by centrifugation at 6000g for 10 min. The pellet was resuspended in 15 ml 200 mM Tris-HCl pH 8.0, 0.65 mM EDTA, 500 mM sucrose per litre pellet and incubated for 1 h on ice. Followed by the addition of 30 ml of 200 mM Tris-HCl pH 8.0, 0.65 mM EDTA, 125 mM sucrose, the cells experience an osmotic shock and release proteins from the periplasm. After an additional hour on ice, the cells were centrifuged for 45 min at 12 000g. The periplasmic extract was incubated with cobalt-loaded beads (Talon Metal Affinity Resin, Clontech) for 30 min and poured into an empty column (PD10, GE Healthcare). After washing with 10 CV 50 mM Na<sub>2</sub>HPO<sub>4</sub>/NaH<sub>2</sub>PO<sub>4</sub> pH 7.4,

**Table 2**  
Crystallization.

Method	Sitting drop	Hanging drop
Plate type	96 × 3-well	24-well
Temperature (K)	293	293
Protein concentration (mg ml <sup>-1</sup> )	25	25
Buffer composition of protein solution	50 mM Tris pH 8.0, 150 mM NaCl, 2 mM DTT	50 mM Tris pH 8.0, 150 mM NaCl, 2 mM DTT
Composition of reservoir solution	0.1 M sodium cacodylate pH 5.5, 25%(w/v) PEG 4000	0.1 M Tris pH 8.5, 15%(w/v) PEG 6000
Volume and ratio of drop	100 nl (1:1 ratio)	1 µl (1:1 ratio)
Volume of reservoir (µl)	70	200

300 mM NaCl, 5 mM imidazole, the nanobody was eluted with 4 CV of 50 mM Na<sub>2</sub>HPO<sub>4</sub>/NaH<sub>2</sub>PO<sub>4</sub> pH 7.4, 250 mM NaCl, 250 mM imidazole. To polish the nanobody and exchange the buffer, concentrated nanobody was injected onto a Superdex 75 HR 16/60 column equilibrated with 50 mM Tris pH 8.0, 150 mM NaCl, 2 mM DTT. The nanobody-containing fractions were concentrated (Amicon Ultra, MWCO 3000, Millipore) to a minimal concentration of 10 mg ml<sup>-1</sup> and stored at 253 K.

### 2.1.3. Preparation of the GasAHD in complex with a nanobody.

To prepare a 1:1 GasAHD–CA9177 complex, purified GasAHD was mixed with a 1.2 molar excess of CA9177 and incubated for 1 h. The complex was purified from free nanobody using a Superdex 75 HR 16/60 column equilibrated with 50 mM Tris pH 8.0, 150 mM NaCl, 2 mM DTT (Fig. 1a). Fractions containing the GasAHD–CA9177 complex were pooled and concentrated (Amicon Ultra, MWCO 3000, Millipore) to 40 mg ml<sup>-1</sup> and verified by SDS–PAGE (Fig. 1b). On the SDS–PAGE gel, GasAHD (123 amino acids) and CA9177 (121 amino acids) run at molecular masses of 14.7 and 13.4 kDa, respectively.

## 2.2. Crystallization

The initial crystallization trials consisted of one commercial screen: ProPlex HT-96 (Molecular Dimensions). The crystallization screen was set up using a Phoenix crystallization robot (Art Robbins Instruments): three different protein concentrations (35, 25 and 15 mg ml<sup>-1</sup>) were dispensed into three-well Intelli-Plate 96 plates (Hampton Research). For the sitting-drop vapour-diffusion method, 100 nl of screening solution was mixed with an equal volume of

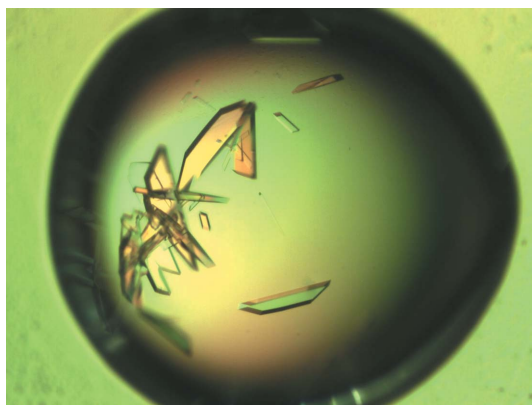


**Figure 2**  
GasAHD–CA9177 crystals. Crystals of GasAHD–CA9177 obtained after streak-seeding in 0.1 M Tris pH 8.5, 15%(w/v) PEG 6000. Crystals were grown in 1 d using the hanging-drop method in 24-well plates.

**Table 3**  
Data collection and processing.

Values in parentheses are for the outer shell.	
Diffraction source	PROXIMA-1, SOLEIL
Wavelength (Å)	0.9793
Detector	PILATUS 6M
Space group	<i>P</i> <sub>2</sub> <sub>1</sub>
<i>a</i> , <i>b</i> , <i>c</i> (Å)	44.07, 52.55, 52.66
$\alpha$ , $\beta$ , $\gamma$ (°)	90.00, 107.89, 90.00
Resolution range (Å)	38.51–1.59 (1.68–1.59)
Total No. of reflections	100990
No. of unique reflections	30170
Completeness (%)	98.3 (94.8)
Multiplicity	3.3 (3.3)
$\langle I/\sigma(I) \rangle$	6.9 (2.1)
$R_{\text{merge}}^{\dagger}$	0.095 (0.641)
$R_{\text{meas}}^{\ddagger}$	0.113 (0.760)
$R_{\text{p.i.m.}}^{\S}$	0.061 (0.405)
Overall <i>B</i> factor from Wilson plot (Å <sup>2</sup> )	11.9

$$\dagger R_{\text{merge}} = \frac{\sum_{hkl} \sum_i |I_i(hkl) - \langle I(hkl) \rangle|}{\sum_{hkl} \sum_i I_i(hkl)}, \quad \ddagger R_{\text{meas}} = \frac{\sum_{hkl} \{N(hkl) / [N(hkl) - 1]\}^{1/2} \sum_i |I_i(hkl) - \langle I(hkl) \rangle|}{\sum_{hkl} \sum_i I_i(hkl)}, \quad \S R_{\text{p.i.m.}} = \frac{\sum_{hkl} \{1 / [N(hkl) - 1]\}^{1/2} \sum_i |I_i(hkl) - \langle I(hkl) \rangle|}{\sum_{hkl} \sum_i I_i(hkl)}.$$

protein solution and the reservoir consisted of 70 µl of the screening solution. The plates were stored at 293 K and crystals appeared in 75% of the conditions after 1 day. Crystals for data collection were harvested from condition C7 [0.1 M sodium cacodylate pH 5.5, 25%(w/v) PEG 4000] and were flash-cooled in liquid nitrogen without additional cryoprotectant. Other crystals from condition D11 [0.1 M Tris pH 8.5, 15%(w/v) PEG 6000] could be reproduced by streak-seeding into 1 µl hanging drops in 24-well VDX plates (Hampton Research; Fig. 2). The PEG 6000 concentration was varied from 10 to 18% in 2% increments. These crystals were harvested and flash-cooled in liquid nitrogen with 0.1 M Tris pH 8.5, 15%(w/v) PEG 6000, 20% glycerol as a cryoprotectant. Crystallization conditions are summarized in Table 2.

## 2.3. Data collection and preliminary X-ray analysis

For data collection, a crystal from the screening plate (ProPlex HT-96 condition C7) was tested without the addition of cryoprotectant. Diffraction data were collected on the PROXIMA-1 beamline at the SOLEIL synchrotron, Paris, France. Data were processed with XDS (Kabsch, 2010). The crystal diffracted to a resolution of 1.59 Å (Fig. 3a) and belonged to the monoclinic space group *P*<sub>2</sub><sub>1</sub>. The unit-cell parameters are consistent with one GasAHD–CA9177 complex per asymmetric unit, with a Matthews coefficient of 2.07 Å<sup>3</sup> Da<sup>-1</sup> and an estimated solvent content of 40.69% (Matthews, 1968). Data-collection statistics are given in Table 3. The structure was solved by molecular replacement using *Phaser* (McCoy *et al.*, 2007) using as input model the helical domain of Gas (PDB entry 3c16; Mou *et al.*, 2009) and the structure of a nanobody based on sequence identity (PDB entry 3p0g; Rasmussen, Choi *et al.*, 2011). The sequence identity between GasAHD and 3c16 is 100% and that between CA9177 and 3p0g is 70%. A solution was found for each search template with a rotation-function Z-score (RFZ) of 44.2 and a translation-function Z-score (TFZ) of 27.6 for 3c16 and an RFZ of 12.9 and a TFZ of 21.1 for 3p0g.

## 3. Results and discussion

Nanobody CA9177 was selected for binding the helical domain of Gas. The GasAHD–CA9177 complex was purified to homogeneity (Fig. 1). Interestingly, using one sparse-matrix screen (ProPlex HT-96), crystals could be grown in about 75% of the conditions tested in

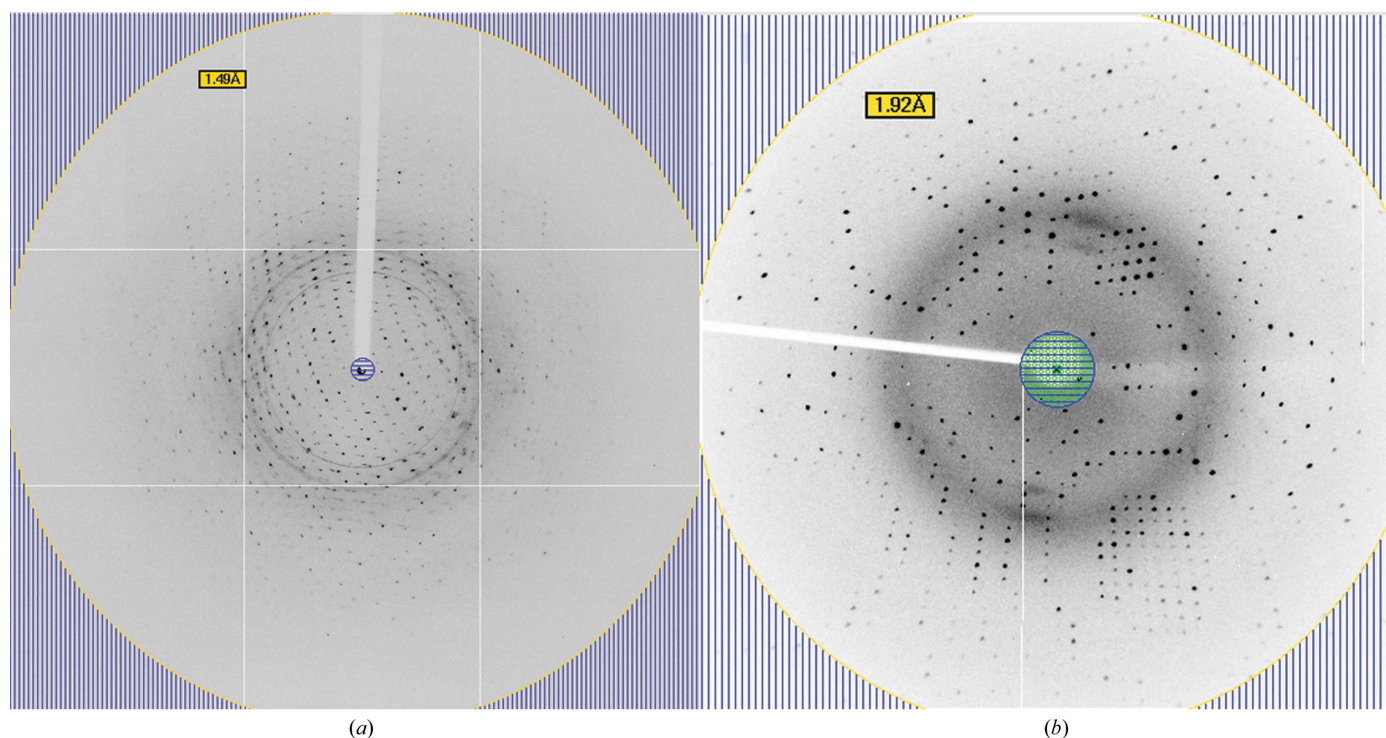


**Figure 3**

Data collection. (a) X-ray diffraction pattern of a GasAHD-CA9177 complex crystal obtained using a synchrotron-radiation source without cryoprotectant. (b) X-ray diffraction pattern using cryoprotectant [0.1 M Tris pH 8.5, 15% (w/v) PEG 6000, 20% glycerol] obtained on a Rigaku MicroMax-007 HF.

24 h. One crystal from condition C7 of ProPlex HT-96 was cooled in liquid nitrogen without cryoprotectant and a high-resolution data set was collected at a synchrotron-radiation source. Ice rings did not hamper data processing, as shown in the data-collection statistics (Table 3). However, another crystallization condition (D11) was reproduced and optimized (Fig. 2), and the crystals diffracted to high resolution (1.9 Å) on a Rigaku MicroMax-007 HF (Fig. 3b). The structure was solved from the synchrotron data set using molecular replacement with PDB entries 3c16 and 3p0g as search models. The CDR (complementary-determining regions) loops of CA9177 were manually rebuilt using *Coot* (Emsley & Cowtan, 2004), followed by several rounds of refinement using *REFMAC5* (Murshudov *et al.*, 2011), giving an *R* factor and *R*<sub>free</sub> of 0.18 and 0.19, respectively, in the final round of refinement.

The structure reveals in detail the epitope recognized by CA9177 on the GasAHD and will prove useful for crystallizing GPCR-G-protein complexes.

This work was supported by the Fonds Wetenschappelijk Onderzoek-Vlaanderen through research grant G.0068.14N and a personal doctoral fellowship to ST, by Innoviris Brussels through the Impulse Life Science Program BRGEOZ132, by the Belgian Federal Science Policy Office through IAP7-40 and by the SBO program IWT120026 from the Flemish Agency for Innovation by Science and Technology. We acknowledge the staff of the PROXIMA-1 beamline at the SOLEIL synchrotron (Saint-Aubin, France) and Dr Lionel Vercheval for their assistance in data collection. We are grateful to Dr Nicolas Villaneuva from Roger Sunahara's laboratory for providing the GasAHD clone.

## References

- Bohm, A., Gaudet, R. & Sigler, P. B. (1997). *Curr. Opin. Biotechnol.* **8**, 480–487.
- De Genst, E. J., Guillems, T., Wellens, J., O'Day, E. M., Waudby, C. A., Meehan, S., Dumoulin, M., Hsu, S.-T. D., Cremades, N., Verschueren, K. H. G., Pardon, E., Wyns, L., Steyaert, J., Christodoulou, J. & Dobson, C. M. (2010). *J. Mol. Biol.* **402**, 326–343.
- Emsley, P. & Cowtan, K. (2004). *Acta Cryst. D* **60**, 2126–2132.
- Hamm, H. E. (1998). *J. Biol. Chem.* **273**, 669–672.
- Irannejad, R., Tomshine, J. C., Tomshine, J. R., Chevalier, M., Mahoney, J. P., Steyaert, J., Rasmussen, S. G. F., Sunahara, R. K., El-Samad, H., Huang, B. & von Zastrow, M. (2013). *Nature (London)*, **495**, 534–538.
- Irannejad, R. & von Zastrow, M. (2014). *Curr. Opin. Cell Biol.* **27**, 109–116.
- Kabsch, W. (2010). *Acta Cryst. D* **66**, 133–144.
- Kruse, A. C. *et al.* (2013). *Nature (London)*, **504**, 101–106.
- Matthews, B. W. (1968). *J. Mol. Biol.* **33**, 491–497.
- McCoy, A. J., Grosse-Kunstleve, R. W., Adams, P. D., Winn, M. D., Storoni, L. C. & Read, R. J. (2007). *J. Appl. Cryst.* **40**, 658–674.
- Mou, T.-C., Masada, N., Cooper, D. M. F. & Sprang, S. R. (2009). *Biochemistry*, **48**, 3387–3397.
- Murshudov, G. N., Skubák, P., Lebedev, A. A., Pannu, N. S., Steiner, R. A., Nicholls, R. A., Winn, M. D., Long, F. & Vagin, A. A. (2011). *Acta Cryst. D* **67**, 355–367.
- Muyldermans, S. (2013). *Annu. Rev. Biochem.* **82**, 775–797.
- Muyldermans, S., Cambillau, C. & Wyns, L. (2001). *Trends Biochem. Sci.* **26**, 230–235.
- Oldham, W. M. & Hamm, H. E. (2008). *Nature Rev. Mol. Cell Biol.* **9**, 60–71.
- Pardon, E., Laeremans, T., Triest, S., Rasmussen, S. G. F., Wohlkönig, A., Ruf, A., Muyldermans, S., Hol, W. G. J., Kobilka, B. K. & Steyaert, J. (2014). *Nature Protoc.* **9**, 674–693.
- Rasmussen, S. G. F., Choi, H.-J. *et al.* (2011). *Nature (London)*, **469**, 175–180.
- Rasmussen, S. G. F., DeVree, B. T. *et al.* (2011). *Nature (London)*, **477**, 549–555.
- Simon, M. I., Strathmann, M. P. & Gautam, N. (1991). *Science*, **252**, 802–808.
- Steyaert, J. & Kobilka, B. K. (2011). *Curr. Opin. Struct. Biol.* **21**, 567–572.
- Westfield, G. H. *et al.* (2011). *Proc. Natl Acad. Sci. USA*, **108**, 16086–16091.